Composites: Part A 167 (2023) 107450

Contents lists available at ScienceDirect

Composites Part A

journal homepage: www.elsevier.com/locate/compositesa

A critical appraisal of fracture mechanics methods for self-healing and healable composites characterization

F. Benazzo [a,b], D. Rigamonti [a], G. Sala [a], A.M. Grande [a,*]

[a] Department of Aerospace Science and Technology, Politecnico di Milano, Milano, via la Masa 34, 20156 Milano, Italy
[b] Graduate Aerospace Laboratory, California Institute of Technology, 1200 E. California Blvd., Pasadena, CA 91125, USA

ARTICLE INFO

Keywords:
Healing efficiency
Delamination
Mechanical testing
Interlaminar fracture toughness

ABSTRACT

Self-healing and healable Fibre Reinforced Polymer composites (FRPs) have tremendous potential in reducing the weight and increasing the lifetime of aerospace structures. While several strategies have been developed to add healing functionality to composites, there is no generally accepted method for the evaluation of their healing efficiency. Most testing approaches are based on interlaminar fracture toughness evaluation which revolves around three widely recognised methods: double-cantilever beam (DCB), three-point end-notch flexure (3-ENF), and four-point end notch flexure (4-ENF) testing. Alternative tests also employed in literature are low-impact velocity, micro-cutting, and short-beam shear (SBS) testing. This paper introduces the advantages and disadvantages of each test method when applied to healing FRPs while highlighting and explaining the large inconsistencies found among investigations. Ultimately, this review provides the necessary tools in choosing the most adequate test method for the characterization of a novel mendable FRP.

1. Introduction

The application of fibre-reinforced polymer (FRPs) composites is now commonplace in almost every field of engineering, ranging from aerospace and naval structures to the civil and automotive industry. As a result, considerable progress is being made on the technological advancements in the manufacturing and material properties of composites may benefit a countless number of applications, and thus considerable achievements are being made [1–3]. For instance, investigations are being conducted to develop manufacturing techniques for the reinforcement and matrix phases of composites, along with their respective combinations, in order to improve mechanical properties. Novel research is also being conducted to implement a number of functionalities to FRPs, such as the development of composites with shape memory [4,5], energy storage [6], morphing and multi-stability [7–9], piezoelectric [10,11], reprocessing [12], or sensing capability [13–16] and damage healing [17,18]. The latter comprises FRPs with a standard reinforcement phase, i.e., carbon or glass fibres, combined with a self-healing or healable polymeric matrix phase. This mending capability would potentially increase the lifetime of the composite, while maintaining the excellent properties of fibre composites, namely the low density and tensile strength along the fibres' direction. The growing scientific interest in this family of multifunctional materials is demonstrated in Fig. 1, where the evolution of the volume of literature studies focused on FRPs and healing composites is compared. Here, the increment in the yearly publications of the two sets since 2010 to today shows that healable composites have drawn considerably more resources and focus.

All of the healing polymers used in the studies presented in Fig. 1 may be classified depending on the chemical or physical route used to repair the micro-cracks present in the material. Mimicking biological systems is one approach to repairing defects and is achieved through one of two referenced methods: extrinsic or intrinsic healing [19–21]. The former involves the integration of microcapsules carrying the healing agent in the matrix phase [22]. When cracked, these capsules release the chemical into the damage site, activating the reaction to reform the broken covalent bonds. Alternatively, microchannels connected to a reservoir of the healing agent can be inserted in the matrix phase and repair damage with a similar working principle [23,24]. Other researchers, such as Azcune and Odriozola [25] and Grande et al. [26] have implemented polymers with reversible dynamic covalent bonds that restore the original material's integrity by activating this reversible capability. This is known as intrinsic self-healing since the healing agent is not embedded in the material as a secondary phase, but as part of the molecular network through reversible bonds. A unique family of

* Corresponding author.
E-mail address: antoniomattia.grande@polimi.it (A.M. Grande).

https://doi.org/10.1016/j.compositesa.2023.107450
Received 20 September 2022; Received in revised form 11 January 2023; Accepted 13 January 2023
Available online 18 January 2023
1359-835X/

Nomenclature

3-ENF	3-point end notch flexure
4-ENF	4-point end notch flexure
5%/Max	5% offset/maximum load
DCB	double cantilever beam
DDS	diamino-diphenyl sulfone
DMP-30	2,4,6-Tris (dimethylaminomethyl) phenol
DGEBA	Bisphenol A diglycidyl ether
EMAA	poly(ethylene-co- methacrylic acid)
EPA	Ethyl phenylacetate
FRP	fibre-reinforced polymer composite
G, G_I, G_{II}, G_{III}, G_C	energy release rate (for mode I, II, and III) and the critical energy release rate
MWCNTs	Multi-Wall Carbon Nanotubes
NL	non-linear
PCL	polycaprolactone
PET	polyethylene terephthalate
PETMP	pentaerythritol tetrakis(3-mercaptopropionate)
PIPS	polymerisation-induced phase separation
PLA	polylactic acid
SBS	short-beam shear
VIS	visual observation

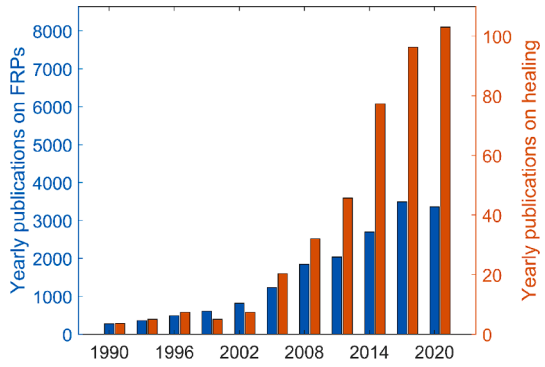

Fig. 1. Number of published articles on a three-year average that focused on FRPs and healable composite materials, presented in blue and orange respectively (data gathered from Scopus search). (For interpretation of the references to colour in this figure legend, the reader is referred to the web version of this article.)

intrinsically healed matrices are thermoplastic polymers, which tend to be embedded in the interlaminar region [27,28], and heal matrix damage through thermo-reversible secondary bonds, such as hydrogen-bonds [29].

Composites with healable matrices may become an optimal alternative to traditional FRP matrices due to their potential to lower safety factors, since small damages and cracks that are predicted to degrade the material properties can be repaired. In fields of engineering where weight is crucial, such as the aerospace industry, lower safety factors lead to considerable cost savings [30–32] and depending on the confidence and the reproducibility of the repair mechanism mendable materials may be in service for several more loading cycles than similar composites due to the slower or theoretically inexistent degradation.

Given the increasing interest in these promising capabilities of multifunction materials, a common and internationally recognized testing method is required to adequately compare the healing performance of this novel FRP family. Despite a recent study [33] demonstrating a considerable degree of healing at the fibre–matrix interface, the healing functionality is generally related to the matrix phase. Thus, the tests employed to evaluate the healing efficiency of novel FRPs must measure the strength of the matrix phase before and after being subjected to both damage and its unique healing process. In addition, the deterioration created during the test must be controlled and monitored in order to replicate the failure mode that these multifunctional materials attempt to tackle, commonly delamination and microcracking. More substantial damage would indeed be impossible to mend with the majority of extrinsic and intrinsic healing systems And if large deformations occur in specimens showing fibre bridging, the fibres' new position and misalignment after reparation may hinder healing functionality entirely.

Bearing these aspects in mind, the most appropriate mechanical property to compare virgin and healed FRP specimens is delamination, which involves the controlled cracking of the matrix phase. The quantitative measure for delamination is interlaminar fracture toughness, also known as the energy necessary to propagate an interlaminar crack in a composite. Several mechanical tests, including double cantilever beam (DCB) and end notch flexure (ENF), can measure fracture toughness. However, the differences in the apparatus and specimens employed in these tests do not allow for the comparison of results between testing methods. As a result, the principal difficulty encountered while comparing recent studies and comprehensive review papers [34,35] on the mechanical characterization of healable and self-healing FRPs was the lack of a standard method to determine the ability to restore delamination resistance of these systems. Therefore, the foremost objective of this review is to provide the reader with an understanding of the benefits and drawbacks of the test methods used in the investigations. A secondary objective is to establish the foundations to create a common set of testing procedures for self-healing and healable FRPs that will enable to confidently compare their mending abilities and evaluate the performances of the healing matrix phase.

Considering these intents, the structure of the paper is as follows. Section 1.1 considers fracture toughness tests in their application to studies concerning healing materials. Section 2 includes detailed descriptions of the methods and procedures of the mechanical tests and incorporates evaluations on the appropriateness of the tests to the current studies on healing composites. Three widely used tests that measure interlaminar fracture toughness have been discussed: DCB, 3-point end notch flexure (3-ENF), and 4-point end notch flexure (4-ENF). Testing methods such as short-beam shear (SBS), low-velocity impact testing and micro-cutting testing, which have also been incorporated in some studies to characterize self-healing and healable composites, are also summarized. Finally, sections 3 and 4 compare these testing methods in discussions strictly related to healable FRPs.

1.1. *Interlaminar fracture toughness tests with healable FRPs*

Several research studies on healable composites, reported in Table 1, adopted fracture toughness tests to evaluate healing performance, but their conclusions on the degree of repair of each healing approach may not be properly compared before a thorough analysis of the main characteristics that distinguish fracture toughness tests from other more common mechanical tests is performed. In general, delamination tests observe cracks' development along the interlaminar layer during the loading of the specimens. Interlaminar cracks are achieved by either introducing opposing stresses in adjacent layers – ENF tests rely on the contemporary compression of the top layers and tension of the bottom layers – or tearing apart of the layers – DCB tests involve the vertical deformation of the top and bottom halves in opposite directions. The difficulty in controlling the location and manner of interlaminar fracture onset requires the implementation of inserts to act as crack initiators.

The materials, healing method, and test method of each investigation listed in Table 1, along with the detailed evaluation of the aspects of the specific tests, provide essential tools for an adequate comparison between healing efficiencies. The comparison of these aspects that follows in the next sections demonstrates how a unique testing procedure is

Table 1
Fracture toughness tests with self-healing materials.

Reinforcement	Healing material	Healing method	Healing approach	Test method	Heling efficiency	Reference
Glass fibre	DCPD monomer with Grubb's catalyst	microcapsules	Extrinsic	DCB	20%	[36]
Carbon fibre	DCPD monomer with Grubb's catalyst	microcapsules	Extrinsic	DCB	73%	[41]
Glass fibre	DGEBA with CuBr2(2-MeIm)4 catalyst	microcapsules	Extrinsic	DCB	79%	[42]
Glass fibre	EMAA copolymer	healing adhesive	Intrinsic	DCB	88%	[43]
Carbon fibre	EMAA copolymer	healing adhesive	Intrinsic	DCB/3ENF	411%/100%	[37]
Carbon fibre	EMAA copolymer	healing adhesive	Intrinsic	DCB	310%	[44]
Glass fibre	EPA and DGEBA with Sc(OTf)3 catalyst	microvascular	Extrinsic	DCB	352%	[45]
Glass fibre	EPA and DGEBA with Sc(OTf)3 catalyst	microcapsules	Extrinsic	DCB/3ENF	0%/10%	[46]
Carbon fibre	Monomer 400/401	healing adhesive	Intrinsic	DCB	0%	[47]
Glass fibre	NM 275A with NM275B hardener	microvascular	Extrinsic	3ENF	40%	[48]
Carbon fibre	C1.5DA1T and C2DA1H resins	dynamic bonds	Intrinsic	SBS	85%	[49]
Carbon fibre	SPSH01	healing adhesive	Intrinsic	3ENF	>100%	[50]
Carbon fibre	SPSH01	healing adhesive	Intrinsic	DCB	59%	[51]
Carbon fibre	EMAA copolymer	healing adhesive	Intrinsic	DCB	60%	[52]
Carbon fibre	PETMP and DMP30 in DGEBA	microcapsules	Extrinsic	DCB	80%	[53]
Carbon fibre	BMI based polymer	dynamic bonds	Intrinsic	DCB	30%	[54]
Carbon fibre	Sc(OTf)3	microcapsules	Extrinsic	DCB	44%	[55]
Carbon fibre	MWCNT's in DGEBA and EPA matrix	microvascular	Extrinsic	DCB	192%	[38]
Carbon fibre	PETMP and DMP30 healing agents in DGEBA resin	microcapsules	Extrinsic	3ENF	57%	[56]
Glass fibre	PCL healing agent in DGEBA and DDS hardener	dynamic bonds	Intrinsic	DCB	60%	[57]
Carbon fibre	poly(lactic acid) film	healing adhesive	Intrinsic	DCB/4ENF	N/A	[58]
Carbon fibre	DGEBF and TDI with ISOX	dynamic bonds	Intrinsic	SBS	85%	[59]
Carbon fibre	L/EPH 161 resin with copolymer nylon Griltex D 1330A as MWCNT	dynamic bonds	Intrinsic	DCB/3ENF	96%/86%	[39]
Carbon fibre	PCL healing agent with SMA dispersion	dynamic bonds	Intrinsic	DCB	73%	[60]
Glass fibre	CNT and EMAA	healing adhesive	Intrinsic	DCB	129%	[61]
Carbon fibre	PCL healing agent in DGEBA and aliphatic amine hardener	dynamic bonds	Intrinsic	DCB	146%	[62]
Carbon fibre	EMAA copolymer	healing adhesive	Intrinsic	DCB	76%	[63]
Carbon fibre	EMAA copolymer	healing adhesive	Intrinsic	DCB	185%	[27]
Carbon fibre	EMAA copolymer	healing adhesive	Intrinsic	DCB	143%	[64]
Carbon fibre	L/EPH 161 resin with copolymer PET as MWCNT	dynamic bonds	Intrinsic	DCB/3ENF	9%/140%	[40]
Carbon fibre	L/EPH 161 with DGEBA with Sc(OTf)3 as healing agent	microcapsules	Extrinsic	3ENF	84%	[65]
Carbon fibre	Loctite 480 healing agent	microvascular	Extrinsic	DCB/4ENF	240%	[66]
Carbon fibre	PCL healing agent in DGEBA and aliphatic amine hardener	dynamic bonds	Intrinsic	3ENF	96%	[67]
Glass fibre	poly(borosiloxane) layers	healing adhesive	Intrinsic	DCB	100%	[68]
Glass fibre	SIROPOL 8330 polyester resin	syringe delivered agent	Extrinsic	DCB	101%	[69]
Carbon fibre	CF-PA6 thermoplastic sheets	healing adhesive	Intrinsic	DCB	91%	[70]
Glass fibre	DGEBA with vitrimer resin 4-AFD	dynamic bonds	Intrinsic	4ENF	95%	[71]
Carbon & glass fibre	EMAA copolymer	healing adhesive	Intrinsic	DCB	82%	[29]

necessary to adequately pick the most efficient healing system. Indeed, the large number of possible combinations of materials, testing methods and data reduction approaches lead to substantial differences between the healing efficiencies considered, which will be further explored in Sections 3 and 4 of this review.

A series of general remarks can be drawn from the data in Table 1. First, it may be noted that Kessler and White [36], who produced the earliest investigation on this topic, implemented an extrinsic healing system with a microencapsulated repair agent in a glass fibre composite, and thus several more studies with a similar repair mechanism were conducted in the following decades. Extensive characterization was also performed on poly(ethylene-co-methacrylic acid) (EMAA) adhesive strips placed between the central layers of the laminate. These thermoplastic strips could be thermally repaired and were shown to provide very high healing efficiencies – up to 411% [37]. Extrinsic healing through a microvascular network also resulted in reported efficiencies greater than 100%. Other studies attempted to implement both healing and improved mechanical properties, such as Bekas et al. [38] by successfully injecting a self-healing agent with Multi-Wall Carbon Nanotubes (MWCNTs).

The notable high efficiencies reported in many investigations would mean that the material performed better after being damaged and consequently repaired, which is surprising since one would opt to begin the lifespan of a component with its strongest configuration, rather than await its degradation and healing to benefit from the enhanced damage resistance. A reasonable explanation is that through the healing process, the thermoplastic polymers, which have been observed to exhibit these high healing efficiencies, flowed through the cracked matrix and bonded the cracked interface. Thus, a distinction must be made when considering the 1st healing efficiency of these types of healable FRPs and that of healable composites that do not undergo such radical modifications in their microscopic composition during the mending cycles. Nonetheless, this distinction should not undermine thermoplastic mendable systems in the ranking of their performance. For instance, the study from Snyder et al. [29] presented a novel material architecture involving in-situ heating and 3D printing of thermoplastic polymer networks, that allowed for continuously repeatable healing, up to 100 cycles. Such material characteristics should certainly be taken into count by the metric that would classify the healing ability of mendable FRPs.

Another element to notice in Table 1, is that the most common testing method was DCB loading, even though 3-ENF tests were also reasonably popular. A series of studies offered comparisons between self-healing systems tested under both methods and permitted to evaluate the advantages and disadvantages of each approach directly. These comparisons showed that deductions on the results obtained from the two tests were often inconsistent with each other. For instance, Kostopolous et al. [39] found a larger efficiency with DCB testing compared to 3-ENF, while in an ensuing study Kotrotsos and Kostopoulos [40] showed that 3-ENF testing exhibited efficiencies almost 16 times larger than those calculated from mode I testing. These inconsistencies were attributed to the kind of particles dispersed in the matrix phase.

Finally, it can be noticed that most of the healing methods employed

are intrinsic, because of the challenging integration of extrinsic systems in the matrix phase and their complex manufacturing procedures. For example, microcapsule-based systems require the preparation of several components: the microencapsulated healing agent, the microcapsules' shell, the microcapsules-filled solution, and the matrix phase. These are drawbacks that affect cost, time, and applicability of such composites to industry.

2. Test methods

As previously stated, fracture tests aim to determine the energy release rate (G) during delamination. The loading method with which this quantity is measured influences its value and is specified using a subscript following the property's symbol. DCB evaluates mode I failure, which involves the tearing of the layers of the composite apart, and thus measures G_I. ENF tests evaluate mode II failure (G_{II}) and involve the sliding of one layer on the other by flexure [72]. Meanwhile, mode III failure (G_{III}) consists in the lateral sliding of the composite's layers and is rarely explored due to the very high complexity of the testing apparatus and procedure. The following sections enumerate the several differences between the mechanical tests included in Table 1 and provide crucial insights into choosing the appropriate method to characterise healable composites. Certain aspects of the test, such as the stress fields and geometry of the specimens, are briefly summarized in this section and compared in greater detail in Section 3 with the focus shifted to their application to mendable FRPs.

2.1. Double cantilever beam

DCB testing is the most commonly used approach to measure resistance to delamination. Similarly to other fracture toughness tests it requires FRP specimens to incorporate layers stacked on the horizontal plane and separated by an insert, generally made out of a thin sheet of non-adhesive materials, that acts as a crack initiator as described in ASTM standard D5528. Rectangular specimens are also attached to hinges or blocks to transfer the load in a constant vertical direction (Fig. 2) to tear the two halves apart.

Results from DCB tests can be processed relatively quickly and with ease thanks to the readily identifiable stress fields and deformations that occur. The vertical loads determine uniform stress at the crack tip, which leads to the steady propagation of the crack, thus allowing for the creation of an R-curve to represent the relationship between fracture toughness and crack length [73,74]. In addition, the test permits the identification of multiple critical fracture toughness values (G_{IC}): the non-linear (NL) point, the visual observation (VIS) point, and the 5% offset/maximum load (5%/Max), which allow for additional statistical analysis and data comparison, as performed by Jony et al. [75]. For an analytical evaluation of DCB testing, the mode I fracture toughness derivation in polar coordinates by Irwin [76] provides the following integral expression:

$$G_I = \lim_{\Delta a \to 0} \frac{1}{2\Delta a} \int_0^{\Delta a} \sigma_y(\Delta a - r)\bar{v}(r, \pi)dr \quad (1)$$

where the infinitesimally small crack propagation is denoted by Δa, r and π indicate the polar coordinates, σ_y is the normal stress at the origin, and $\bar{v}$ is the displacement of the two central layers.

As a result of the aforementioned advantages, a variety of healable composite investigations make use of this testing method. For example, in their multiple studies on self-healing composites, Cohades et al. [57,77] have gathered data through this test method, and their earliest work will be analysed here in detail to present key aspects of mode I delamination. In the investigation, the healable material is an epoxy resin with three components: the pre-polymer as bisphenol A diglycidyl ether (DGEBA) resin, the hardener as 4,40-diamino-diphenyl sulfone (DDS), and the healing agent as polycaprolactone (PCL), which is a thermoplastic polymer that can be mixed with the epoxy resin. Under specific conditions, PCL can be embedded in the matrix phase through a polymerisation-induced phase separation (PIPS) process and, being a thermoplastic material, PCL can repair composites with the correct thermal process, hence repairing matrix damage.

In this study, two types of healable systems, with different concentrations of thermoplastic polymer (PCL (25) and (37)), were tested under DCB procedure to obtain load–displacement plots as shown in Fig. 3(a). After subjecting the matrix to the healing cycle, which consisted of a heat cycle at 150 °C for 30 min and subsequent cooling to room temperature, the specimens were mechanically tested in the same manner as the virgin state. The G_{IC} values calculated with the Modified Beam Theory prior to healing and post-repair conditions were then compared. At this stage, the healing efficiency was determined with two methods: by the ratio of the stiffness of the specimens calculated from the slopes of the load–displacement linear curves, and by the ratio of the healed G_{IC} to the virgin G_{IC}. In total, three healing cycles were performed and the data from the healing efficiency based on fracture toughness populated the bar graph in Fig. 3(b), where the maximum healing efficiency of 60% was recorded at the 3rd healing cycle. Unlike many other healing materials, epoxy resins containing PCL appeared to heal best after a few healing cycles due to the expansive bleeding mechanism in which PCL is distributed in the FRP during thermally activated healing. Equivalently to EMAA [37], an even distribution of PCL through the matrix' voids may require multiple fractures and healing cycles, reflecting the continuous increase in efficiency over the first few cycles. In the paper, investigators had to attempt different data reduction strategies to determine the healing efficiency, which ultimately yielded differing results. This confirms the need for a single performance metric for healable FRPs, which, in the case of this study, should also account for the thermally induced flow behaviour of the healing agent.

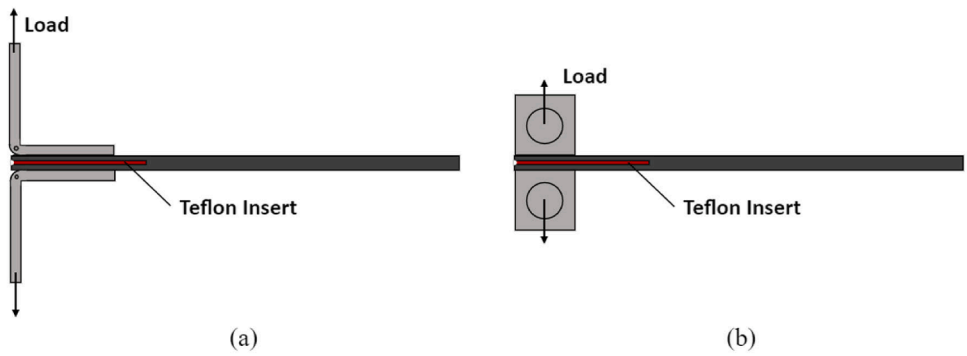

Fig. 2. Example of specimens used for DCB tests with (a) hinges and (b) blocks.

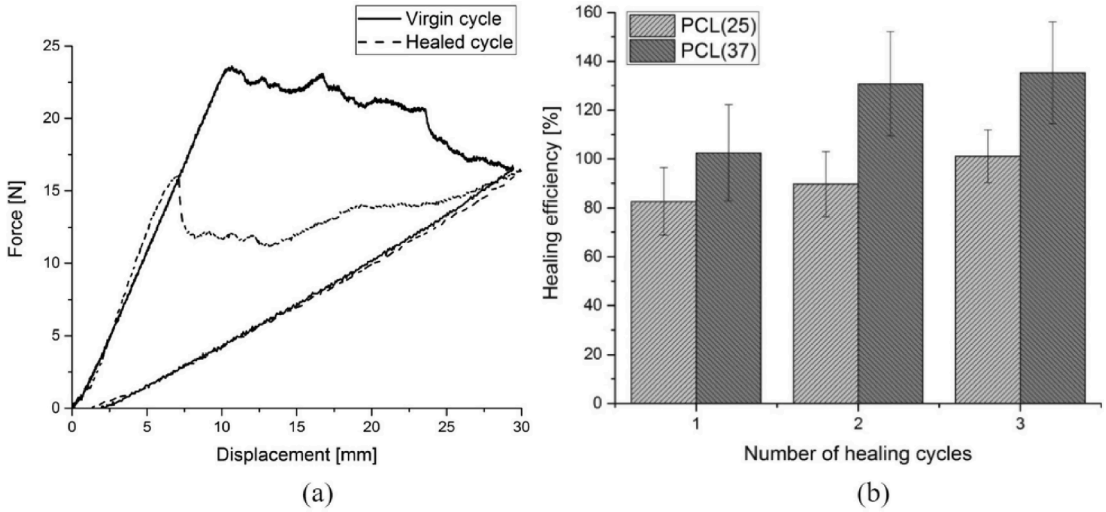

Fig. 3. (a) Load-displacement plot for DCB test and (b) healing efficiency of 3 healing cycles calculated by comparing fracture toughness [57]. Reproduced with permission from Elsevier.

2.2. End notch flexure at three points

3-ENF tests involve bending composite specimens until the crack propagates from the insert's tip to the top loading nose (Fig. 4). This occurs due to the shear stress between the top and bottom layers, caused by opposing compression and tension on the two halves respectively. One aspect of 3-ENF tests that is advantageous to DCB is the simplicity of the specimen's preparation: so long as the rectangular specimen is within the size parameters set by ASTM D7905, it does not require any further modifications, such as the addition of loading blocks or hinges. This failure mode is also more resemblant to the loading that composites in aerospace applications undergo, and thus offers insights into the repair ability of mendable FRPs in real-life conditions. However, the load applied at a single central location of the specimen may determine surface damage on the top layer of some brittle composites, which may require sacrificial layers of rubber, aluminium, or Teflon strips [78–80] to be laid on the surface of the laminate. Finally, a noteworthy aspect of this test is that the bending stress generated in the two halves is non-uniform between the loading pins, causing abrupt advancements of the crack from the insert to the top loading pin and making any observations on the crack propagation behaviour difficult.

The method, presented in ASTM standard D7905 and described during its application in a NASA report by O'Brien et al. [81], is not particularly difficult to perform and takes into account the unstable crack growth by neglecting crack length measurements. The analytical expression for G_{II} (Eq. (2)) is also similar to Eq. (1) [76], yet differs from the latter in the stress (τ_{xy}) acting on the laminate. This shear stress implies that frictional effects influence tests results [82] and may only be mitigated using calibration procedures explained in the ASTM standard. Thus, careful consideration is required when comparing mode II fracture toughness results between dissimilar fibre–matrix combinations.

$$G_{II} = \lim_{\Delta a \to 0} \frac{1}{2\Delta a} \int_0^{\Delta a} \tau_{xy}(\Delta a - r)\bar{u}(r, \pi)dr \tag{2}$$

The above equation employs the same abbreviations as Eq. (1), yet replaces the layers' vertical displacement with their lateral displacement $\bar{u}$.

As a result of its benefits, 3-ENF testing is used in a series of investigations, and, with respect to self-healing FRPs, it was most notably employed by Ghazali et al. [56]. In this study, an epoxy resin matrix phase composed of DGEBA and Araldite-F was healed by a micro-encapsulated healing agent formed by pentaerythritol tetrakis(3-mercaptopropionate) (PETMP) and 2,4,6-Tris(dimethylaminomethyl) phenol (DMP-30) in a 24-hour healing cycle at 4 Bar and 70 °C. The virgin FRP specimens were tested according to the standard, employing the apparatus shown in Fig. 5(a), and repaired through the healing process to be repeatedly mechanically tested. The pre- and post-heling fracture toughness were compared to determine a healing efficiency of 57%, which was attributed to the non-uniform distribution of healing agent in the cracks formed during the fracture test. However, no

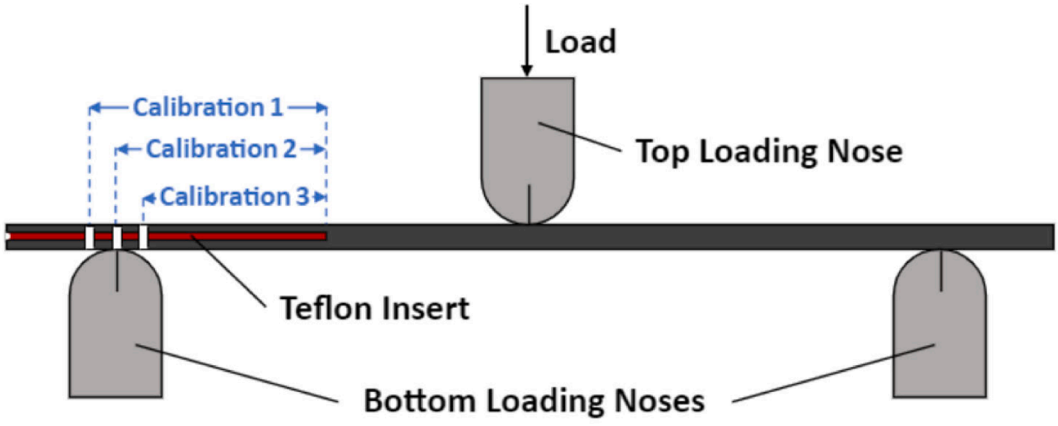

Fig. 4. 3-ENF test set-up according to ASTM standard.

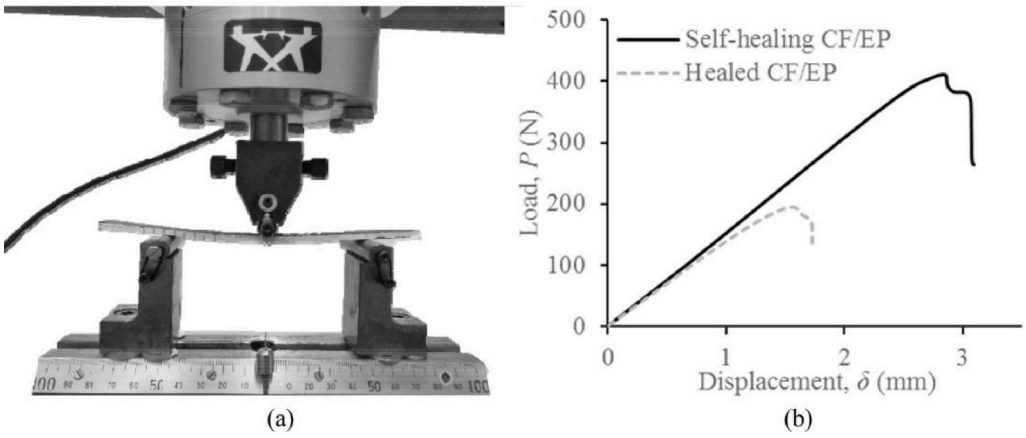

Fig. 5. (a) 3-ENF testing apparatus and (b) load–displacement plot for 3-ENF tests [56]. Reproduced with permission from Elsevier.

conclusions could be drawn on the rate or behaviour of propagation of the crack between virgin and healed specimens due to the unstable crack motion in these ENF tests.

2.3. End notch flexure at four points

Despite several similarities in apparatus between 4 and 3-point ENF tests (Fig. 4 and Fig. 6) the stress distribution and crack propagation in the two are not alike, as inferred from multiple studies [83–85] that compare the two methods. These differences are especially noticeable at the data acquisition and analysis stages of the test procedure.

The instrumentation of the two methods diverges in that 4-point flexure requires a freely rotating top loading block that uniformly distributes the load under two pins [86–88]. This is necessary due to the asymmetrical variation in compliance in the specimen as the crack propagates. With a non-rotating loading block, the vertical displacement of the two top pins would be equal, causing the stiffer side (the one without insert) to undertake most of the load as the stress increases and possibly fail before the desired crack propagation has even begun. The more compliant half indeed requires a larger critical energy for crack initiation and, following the same energy approach explained in section 2.1, this critical energy may only be achieved by vertically deforming it more than the insert-free side. The rotating block ensures a flexible loading distribution on the specimen, and thus a uniform stress in the section of the specimen between the two top pins. As previously explained for the DCB procedure, this uniform bending stress corresponds to the desirable steady crack propagation.

A further consideration that differentiates the ENF tests involves the larger volume of specimen that is under stress in 4-ENF compared to 3-ENF. This aspect implies that there is a greater likelihood of finding flaws and defects in the material and, according to Weibull statistics, the probabilistic certainty of the results is more accurate. Finally, the same considerations as in 3-ENF tests with the existing frictional forces must be noted to indicate the accuracy of the results [83,89].

Despite the advantages of this test method over 3-ENF testing, 4-ENF is not as common as the latter, especially with regard to self-heling FRPs. However, one investigation from Narducci et al. [58] employs this method to characterise the use of polylactic acid (PLA) adhesives in composite specimens. This investigation does not directly evaluate the healing efficiency of the material, but the methodology employed could just as easily be applied to the characterization of repairable FRPs. In their work, Narducci et al. laser cut patches into a carbon/epoxy prepreg (Skyflex^{TM} USN020A), and filled these with PLA, similarly to the integration of EMAA adhesives in other FRPs. Different concentrations of PLA were compared not only quantitatively by calculating mode I and II fracture toughness, but also by observing the load–displacement curves, shown in Fig. 7(a). The crack propagation was also observed in the R-curves shown in Fig. 7(b), ultimately proving that PLA patches would not cause large reductions in fracture toughness, supporting the employment of laser-cut technology to include self-healing thermoplastic materials in FRPs.

2.4. Other methods

One other approach to characterize healable composites is low-velocity impact testing, which has been employed in several research papers [90–98] to substantiate the results of one of the previously described fracture toughness tests. In these tests specimens are generally

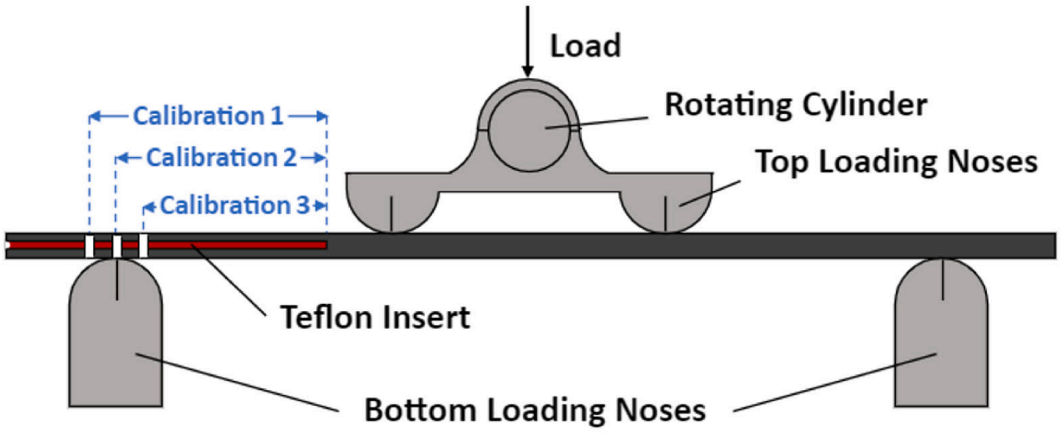

Fig. 6. 4-ENF set-up with pivoting loading point.

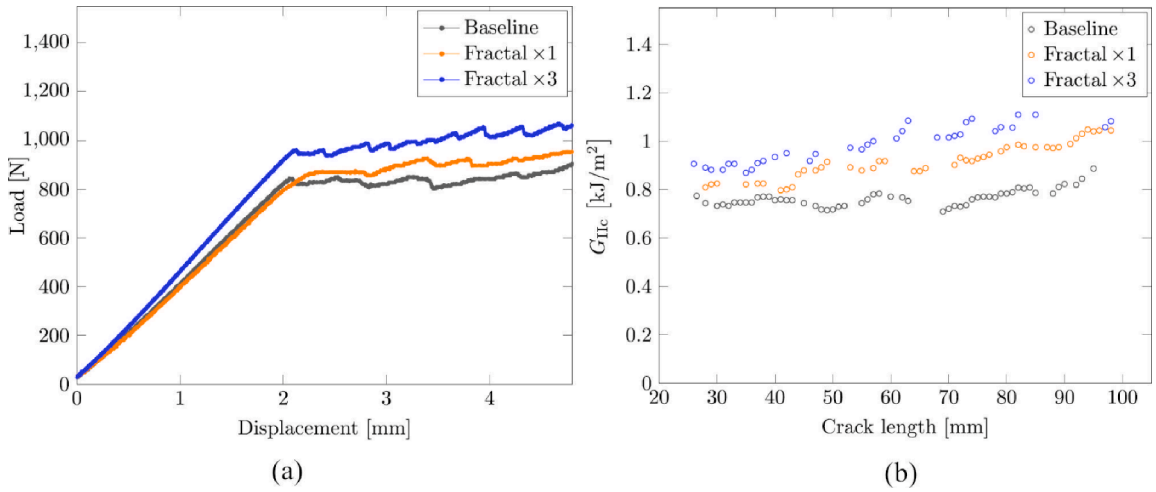

Fig. 7. (a) Load-displacement plot for 4-ENF tests and (b) R-curve determined during 4-ENF test [58]. Reproduced with permission from Elsevier.

plain rectangular laminates held in front of a ballistic target and hit with metallic spheres. The data gathered during the procedure can be analysed to provide the energy absorbed by the material during the impact. However, not all the damage of the collision results in pure delamination and is difficult to link the ability of a material to absorb impact energy with the interlaminar fracture toughness of the matrix phase. This test is a practical tool during early material characterization to visually prove that the healing ability of a resin is effective, although one of the previously mentioned fracture tests would be necessary to quantitatively determine the effectiveness of the healing response for a complete material characterization.

Another novel method to evaluate fracture toughness is micro-cutting testing [99], which employs the use of a sharp cutting edge with an adjustable tool height to apply a force on the composite and, along with parameters regarding the tool's size and cutting angle, the toughness is calculated. The advantages of this test include the ease of production of the specimens and the rapidity of the testing procedure. However, the test requires specific and very accurate machinery and suffers from several inaccuracies attributed to non-perfectly sharp tools or to microscopic defects in the specimen that will determine accidental errors. More importantly, the lack of research performed with this test does not provide the necessary confidence to confirm the repeatability and reliability of the results.

Finally, a similar testing method to 3-ENF called short-beam shear (SBS) testing is relatively common in the literature [49,59,100,101] and involves much smaller, but proportionally thicker specimens aimed at determining the resistance to sliding between layers in composites, rather than the resistance to crack propagation. The test method offers the advantage of requiring smaller specimens, yet the failure mode of the specimen can vary depending on the thickness and brittleness of the composite system. If too thin or ductile, the fibres on the bottom surface will tear, which will cause errors in the evaluation of matrix healing performance. In the optimal failure mode, the interface between layers fails under excessive shear strength and corresponds to a large drop in the load caused by the decreasing stiffness of the material, indicating matrix failure. The test measures strength to failure rather than energy, thus the results cannot be directly compared to DCB or ENF data.

3. Comparison of test methods for healing characterization

This next section aims to summarize and contrast side-by-side the advantages and disadvantages of each test, to provide sufficient information to make an informed decision on the mechanical test to choose in the evaluation of the healing potential of mendable FRPs.

3.1. Dimensions and preparation of specimen

The specimens for the three main testing methods are all rectangular laminates that differ only in dimensions, as per ASTM standards. Notably, the thickness of DCB specimens can significantly vary as the laminate may be much thinner than suggested by ASTM standard and metal plates can be implemented on the top and bottom surfaces to compensate [63,102]. Due to the high cost and complexity of manufacturing most healing matrices, a smaller specimen may be preferable in many investigations. Employing metal plates will systematically affect the results, but, if the objective is to compare the change in fracture toughness before and after a healing cycle to obtain a percent mending efficiency, this modification would be suitable as all measurements are equally affected. Instead, ENF standards require thicker specimens, which correspond to larger quantities of the healing agent. The thickness is directly related to the stiffness, and specimens that are too compliant will not fail under shear during bending, but rather fracture due to concentrated stress applied on the surface. Thin specimens also face excessive flexibility, leading to non-linear behaviours that result in inconclusive outcomes. However, the solution of metal plates is not applicable to ENF tests due to the differences in deformation under bending loads between the composite and the metal, which lead to debonding at the metal-FRP interface. Nonetheless, it is noted that the length of 4-ENF specimens tends to vary more, ranging from 140 [83] to 200 mm [85], and yet still provide comparable results.

It follows that to minimize the volume of healing matrix, the optimal test method would be DCB, Even though this testing procedure is limited by the need for loading hinges and blocks that may hinder the feasibility of the healing process or prevent it altogether from happening. For instance, if the mending cycle requires a uniform pressure on the laminate, it becomes necessary to remove and attach these components to the specimen before and after each healing cycle, which may cause damage to the composite. Furthermore, the bonded interface between the hinges and the specimen is an additional variable in the mechanical test that could lead to inadequate comparisons between results or even become a failure point, rendering test campaigns unsuccessful.

3.2. Test procedures

Mechanical tests' procedures greatly influence the time and resources required to perform testing campaigns, which becomes a significant factor when characterizing novel composites. The correct evaluation of the healing efficiency requires a statistically substantial number of specimens and healing cycles, thus favouring more rapid tests. DCB tests involve a pre-cracking procedure that aims at advancing

the crack from the insert to generate a pure edge crack in the matrix phase. The crack's new location is visually determined, and the full fracture test can be conducted immediately after pre-cracking. Instead, end notch flexure tests involve a set of multiple calibrations at varying crack lengths to determine the compliance coefficients employed in the data analysis. Notably, 4-ENF tests may involve a combination of both pre-cracking and calibration that will slow down the testing process. Again, DCB tests are preferable.

Furthermore, if the investigation is focused on observing the crack propagation through digital imaging of the fracture, it is generally easier to analyse the recordings from DCB tests rather than ENF tests. This is because the fracture of DCB specimens occurs along a constant horizontal line that can be directly analysed with digital image correlation software to monitor the crack's advancement. Instead, ENF tests involve the bending of the majority of the specimen, meaning that the crack becomes a curved line and a more complex software or measuring technique is required to determine the length of the crack. Additionally, the crack tip during DCB testing is effortlessly identified with proper contrast between the specimen and the background. Instead, the sliding of the two halves of the laminate in ENF tests implies that the crack can only be observed where a sufficient gap between the two halves is present.

3.3. Analysis of the stress

Evaluating the stress distribution during each test is crucial to complete a thorough comparison of the testing methods. In DCB the vertical load on the two halves causes a stress concentration at the crack tip, which can be easily modelled as an edge crack [103] propagating when the load reaches the critical value. During the crack's growth the specimen becomes more compliant and, as such, requires a decreasing critical load to propagate the crack, as substantiated by Fig. 3(a), which exhibits a downward sloping curve after the initial peak. Since work performed is equal to half the product of applied load to vertical deformation, to perform more work on the specimen the vertical displacement must be increased. In summary, by continuously deforming the specimen in the vertical direction, the energy increases and reaches a limit at which it is sufficient to propagate the crack in discrete steps, all while the stiffness of the composite decreases due to the ever-larger crack present. Ideally, this process would be continuous with infinitesimally small steps of crack propagation and increase in critical energy G_c, yet imperfections in the material cause a more discrete propagation.

In 3-ENF tests, the force application causes bending stresses that determine the compression of the top half and tension in the bottom half. The uneven deformation of the two parts causes a large stress differential that is maximum in the interface between the middle layers and results in a shear stress. However, there is also a large concentrated axial stress at the centre of the specimen and a bending stress between the two bottom loading pins. This stress distribution means that the critical stress or energy required to propagate the crack is not constant nor increasing as we move farther away from the crack tip. This results in a sudden jump of the crack from the insert tip to its maximum length, which corresponds to the point where the top-loading nose makes contact with the specimen.

In 4-ENF testing the whole volume between the two top pins is under a uniform bending stress, as demonstrated in the work of Lagunegrand et al. [104]. However, the outermost portions of the specimen present stress distributions that are equivalent to 3-ENF loading. The central portion remains under a steady bending stress caused by symmetrical moments at both ends, similar to single halves of DCB specimens. This mixed loading leads to a steady crack propagation only in the central section of the specimen and allows the creation of an R-curve from the test data [84]. Such a crack propagation may be optimal for multi-functional healing composites, as presented by Benazzo et al. [71], where 4-ENF testing allowed to evaluate variations in the crack development of virgin and healed specimens through embedded optical fibres.

The formulation of the measured G in the three main fracture tests also substantiates the behaviour of the crack evolution described above. Equations 3–5 present the relationship between fracture toughness and crack propagation, as derived through the Modified Beam Theory [83,85,89,105]. Since both DCB and ENF tests are regarded as quasi-static mechanical tests, if Equations 3–5 exhibit a right-hand side less than or equal to zero, the crack growth is stable [105].

$$\frac{dG_{DCB}}{da} = \frac{-9\delta^2 E_1 I}{ba^3} \tag{3}$$

$$\frac{dG_{3ENF}}{da} = \frac{-9\delta^2 s^2}{8E_1 b^2 h^3 C^2}\left[1 - \frac{9a^3}{2L^3 + 3a^2}\right] \tag{4}$$

$$G_{4ENF} = \frac{9\delta^2 s^2}{16E_1 b^2 h^3 C^2}\left[1 - \frac{8\mu h}{3s} + \frac{16\mu^2 h^2}{9s^2}\right] \tag{5}$$

$$a \geq L/\sqrt[3]{3} \approx 0.7L \tag{6}$$

In the above formulas, a is the crack length, b is the width of the specimen, h is its thickness, L is the half-length, and s the distance between the first and second loading noses from the left in the 4-ENF apparatus. The geometry and stiffness of the specimens are included in the longitudinal elastic modulus E_1, the moment of inertia about the same axis I, and the material's compliance C. An additional constant term in the 4-ENF equation is μ, which accounts for the frictional effects between the composite layers.

Focusing on the sign of these expressions, one may notice that for DCB toughness the right-hand side is always negative, while further simplifications of the 3-ENF equation is necessary to determine the sign of dG/da. This leads to equation (6), which combined with the technical drawings of 3-ENF specimens in the standard, leads to a dG/da always greater than zero. For 4-point flexure, the calculated G_{II} is independent of crack length, which follows a null dG/da. These observations ultimately concur with the previous claims of a stable crack propagation only in DCB and 4-ENF methods. The recording of this damage propagation is crucial in gaining more insight into the type and extent of interlaminar healing.

The ability to observe the slow progress of the crack also provides better accuracy of the test results. In 3-ENF, the sudden crack motion leads to the conclusion that the maximum load, which is used in the data analysis to determine the fracture toughness, is dependent on the material present just in front of the crack tip, while the response of the matrix between the crack tip and the top loading pin is ignored. This would have not been optimal in the work of Kessler et al. [41], where, thanks to the use of DCB tests, it was deduced that clusters of healing agent filled microcapsules were present in the interlaminar phase. Indeed, the unstable crack growth, which is abnormal for DCB tests, led to believe the presence of a non-homogenous matrix phase that could cause the sudden jumps in crack lengths. Due to the morphology of the studied matrix, this crack growth behaviour was attributed to the inconsistent distribution of the microcapsules [83,106].

3.4. Variation of specimen's geometry and material composition during the healing process

The healing process may also vary the geometry and the microscopic composition of the FRP, consequently diminishing the accuracy of the comparisons between virgin and healed specimens. For example, it was observed by White et al. [22] that the polymerization reaction during the self-healing process could determine the excessive shrinkage of the matrix phase. Alternatively, Manfredi et al. [46] explained that one key factor in the healing process of ethyl phenylacetate (EPA) is the difference in the coefficient of thermal expansion between the healing agent and resin. This resulted in the expansive bleeding mechanism, also

observed with PCL by Cohades and Michaud [57], which distributed the substance in the cracks caused by the delamination process. This swelling and shrinking of the matrix phase may cause the formation of flaws and, in the worst-case scenario, interfacial and surface defects. These phenomena determine difficulties for ENF tests which require flat surfaces for the loading pins to properly transfer the loads. Otherwise, the specimens might slip under the large compression and cause inaccuracies in the results during the comparison of healed and virgin samples. Furthermore, the creation of unrepairable defects in the matrix before or after healing could determine a more compliant path for crack propagation, which may hinder the maximum theoretical healing performance [71].

Microcapsules can also greatly affect the microscopic composition of the matrix phase. As observed by Bolimowski et al. [55] the rapture of the microcapsules may lower the fracture toughness due to the increase in porosity corresponding to the emptying of the capsules. However, it was also observed by Ghazali et al. [56] that the decreased density resulting from the increase in voids causes an rise in compliance. Larger compliance generally determines an increase in fracture toughness as the material requires more energy to have the crack propagate. Finally, the leftover debris from the brittle walls of the microcapsules that may remain on the crack interface results in a larger energy to overcome when attempting to develop the crack. As hypothesised and observed by Manfredi et al. [46], this will determine a larger fracture toughness. These factors that arise from the employment of microcapsules equally affect all testing methods, even though ENF tests could present more inaccuracies in the results due to residual debris with respect to DCB testing. Indeed, the debris may cause unwanted frictional forces that were not present in the virgin specimens and influence the fracture toughness of the healed specimens. It has to be noted that the effects of this debris may be detrimental to the delamination resistance of the FRP and, thus, a test method that is capable of observing such influence could be beneficial for a more detailed material characterization.

Other healing approaches could also influence the mechanical properties of the matrix or reinforcement phase after the mending process. This was observed by the work of Brown et al. [106], where the healing agent reacted with the cured polymer in one of the tested mixtures. As a result, the curing agent did not take part in the chemical process intended to repair the damaged matrix, but rather contributed to the formation of inhomogeneities in the material and nullified the healing ability of the polymer.

Finally, many healing processes determine an increase in the thickness of the interface between the composite layers where delamination occurred. For example, PCL and EMAA-based healing takes place through the expansive bleeding mechanism, while extrinsic healing methods, such as microvascular networks, involve the filling of those same gaps by a healing agent. The resulting increase in thickness has been observed by Kessler et al. [41] to cause a considerable decrease in mode I fracture toughness, thus affecting the comparison before and after the healing process. Similar difficulties can be found in intrinsically healed FRPs where the healing moieties are part of the polymer chains that make up the matrix phase. As observed by Heo and Sodano [49], the elevated temperatures of the healing process may determine the activation of undesirable chemical reactions that will form more crosslinks and thus modify the interface or matrix phase. Alternatively, the reactions' by-products may be gaseous and form bubbles in the composite. Both occurrences may affect the thickness and the properties of the central interface ultimately influencing the fracture toughness.

3.5. Fibre bridging

Fibre bridging occurs when fibres of adjacent layers remain connected and cause additional resistance when the two halves of the specimen are being separated. It has been observed in normal FRPs by Gentile [107] and also in healable FRPs by Kessler and White [36], Yin et al. [42], and Kato et al. [66]. Fibre bridging greatly affects the fracture toughness of the laminate and it generally only takes place in the virgin specimen. In the healed samples the crack normally propagates through the same region as in the virgin specimens, and, as the fibres that caused bridging in those locations are already broken or dislocated, there is a lower resistance to damage propagation. As presented by Elhadary et al. [69], where a 12.4% average difference in healing efficiency between non-bridging and bridging specimens was calculated, this phenomenon mainly affects DCB tests where the separation between layers is larger than ENF tests and thus bridging fibres are pulled further apart, suffering more damage.

3.6. Application to real-life conditions

As stated in the introduction, the testing methods measure different fracture toughness, namely mode I through DCB and mode II through ENF, which correspond to alternative types of separation of the composite's layers. These modes of interlaminar damage are representative of ways in which composite materials implemented in engineering systems may fail under load. Therefore, it is useful to understand the most frequent loading modes in the application where composites are more likely to be utilized. Due to the vast number of fields where this class of materials is employed, this evaluation focuses on one industry where composites have been a technological turning point, the aerospace industry.

Three main situations where delamination may occur can be identified in aerospace composite structures. Firstly, fuselages of commercial aviation planes are now made of composite panels or sections that undergo pressurization cycles during each flight. The circular cross-section of the fuselage leads to the generation of hoop stresses in the composite that, result in shear between the adjacent layers, analogous to mode II loading [108]. Secondly, due to the complexity of the shape of the aircraft's components, parts are often fastened together with rivets or bolts. The integration of these fasteners implies the creation of defects through the composite that affect the reinforcement phase by introducing discontinuities in the fibre weaves and increasing the chance of matrix delamination. Fasteners cause complex stresses in the composite [109,110], which tend to include a mixture of both mode I and II loading. Thirdly, both commercial and military aircraft are subjected to large thermal ranges due to the outside environment, aerodynamic drag, and the heat generated by internal components, such as the propulsion system. The differential thermal deformation between the layers of the skin of the aircraft may introduce shear stresses analogous to mode II delamination in the laminate.

4. Remarks on large inconsistencies between healing efficiencies

Table 1 presents large inconsistencies between the healing efficiency calculated from similar materials that were tested through different methods. As said earlier, the fracture toughness calculated through mode I and mode II fracture should be different, however, the healing efficiencies based on fracture toughness should not vary by large margins. This is the case in the work by Kostopoulos et al. [39], in which the calculated efficiencies were 96% and 86% for DCB and 3-ENF testing respectively, even though others, such as Varley and Parn [37] and Kotrotsos and Kostopoulos [40], displayed a significant divergence from the latter reported values.

These differences could be the result of the data reduction method. For instance, both Manfredi et al. [46] and Cohades and Michaud [57] have opted to determine the healing efficiency using the slopes of the linear portions of the load–displacement plots. With this method, the efficiency indicates the ability of the material to restore stiffness rather than fracture toughness and will cause discrepancies when compared to other repairable systems. An alternative approach was that of Aniskevich et al.[48] who employed the flexural moduli calculated from 3-ENF tests to determine the healing efficiencies. Finally, Bekas et al. [38]

compared all their specimens with the results from one single virgin sample, despite the different manufacturing methods of the specimens.

The healing mechanism itself may also cause large inconsistencies. For instance, microcapsule systems carry many difficulties with them and Kotrotsos and Kostopoulos [40] observed that polyethylene terephthalate (PET) particles decreased the fracture toughness of mode I fracture as they acted as stress concentrators and caused unsteady crack propagation. Instead, in 3-ENF testing, these particles caused continuous deviation of the crack which could not propagate through them. Therefore, the longer and more winding path of the crack determined a larger fracture toughness in 3-ENF tests than DCB tests.

Similarly, EMAA-based matrices exhibit diverging behaviours in mode I and II fracture. As shown by Wang et al. [43] and Varley and Parn [37], EMAA is capable of filling voids associated with cracks and improving adhesion between the reinforcement and matrix phase, thus improving the mode I fracture toughness. However, this material has extremely low resistance to shear and, as a result, 3-ENF specimens show much lower healing efficiencies than DCB.

Finally, the thickness of the delamination interface has opposite effects on fracture toughness. As presented by Kessler et al. [41], the increase in the thickness of this interface, which can be caused by the processes described in section 3.5, determines a considerable degradation in mode I fracture toughness. However, Ghazali et al. [56] have described that the same increase in the interface's thickness causes an improvement in mode II fracture toughness. These opposite effects are caused by the different stresses and deformations taking place in the two tests and due to how the change in the volume of delamination affects the energy required to propagate the crack.

5. Conclusions

Despite the copious testing methods to characterize fracture toughness of composites, there are advantages and disadvantages to all such methods when it comes to self-healing and healable composites. Therefore, it can be difficult to choose one single test if the material investigated is novel, with erratic behaviour, and there is little to no research done to compare the results.

The most popular approach, DCB testing, is straightforward in both the required setup and data analysis. However, these tests may not be the most feasible due to the loading hinges or blocks that must be fixed on the specimens. The addition of these components, which may not be properly attached, can also determine failure ahead of time. Yet, the steady progress of the crack provides crucial insights into the level of repair and healing efficiency of the materials.

3-ENF testing is considerably simpler than DCB in terms of specimens' requirements. Nevertheless, the mode II fracture taking place in the composite consists of bending, axial, and shear stresses that can be difficult to properly identify throughout the specimen. Consequently, the crack propagation is very unstable and does not permit the determination of an R-curve, with the linked loss in information on the behaviour of the crack. Finally, the separation of layers due to sliding is affected by changes in the microscopic composition of some FRPs during their healing processes.

The 4-ENF apparatus has the same advantages as 3-ENF and is also characterised by a more stable crack propagation, similar to DCB. Specimens in 4-ENF tests are not subjected to concentrated stresses at the central loading nose and are less likely to show surface cracks in that loading region prior to crack propagation. The loading mode is also representative of the most common stress distributions that occur in real-life applications, in particular when considering aerospace structures. Nonetheless, the data is affected by interlaminar shearing phenomena and the testing apparatus is more complex than the other two tests.

Of the additional testing methods, SBS tests do not adopt the energy approach and look at the interlaminar shear strength instead. This again neglects important insights that could be observed during the interlaminar crack development. However, the test procedure is rapid and relatively straightforward, making SBS testing an optimal tool to substantiate results from a principal testing campaign. Micro-cutting tests have great potential yet lack in literature and more thorough investigations. Finally, impact tests can provide useful qualitative observations on the level of repair, but the data gathered includes non-linear effects of the reinforcement phase, thus not permitting the characterization of the self-healing matrix phase by itself.

All these distinctions in the testing procedures are reflected in the inconsistencies between the healing efficiencies of many FRPs, even those manufactured with the same healing polymers. This is evidence that a common testing method or set of procedures, along with the relative data reduction analysis, is required to accurately compare self-healing and healable composites.

Declaration of Competing Interest

The authors declare that they have no known competing financial interests or personal relationships that could have appeared to influence the work reported in this paper.

Data availability

No data was used for the research described in the article.

References

[1] Ramanathan T, Abdala AA, Stankovich S, Dikin DA, Herrera-Alonso M, Piner RD, et al. Functionalized graphene sheets for polymer nanocomposites. Nat Nanotechnol 2008;3:327–31. https://doi.org/10.1038/nnano.2008.96.
[2] Yao S-S, Jin F-L, Rhee KY, Hui D, Park S-J. Recent advances in carbon-fiber-reinforced thermoplastic composites: a review. Compos Part B Eng 2018;142:241–50. https://doi.org/10.1016/j.compositesb.2017.12.007.
[3] Coleman JN, Khan U, Blau WJ, Gun'ko YK. Small but strong: A review of the mechanical properties of carbon nanotube–polymer composites. Carbon 2006;44:1624–52. https://doi.org/10.1016/j.carbon.2006.02.038.
[4] Liu Y, Du H, Liu L, Leng J. Shape memory polymers and their composites in aerospace applications: a review. Smart Mater Struct 2014;23:023001. https://doi.org/10.1088/0964-1726/23/2/023001.
[5] Liu Y, Lv H, Lan X, Leng J, Du S. Review of electro-active shape-memory polymer composite. Compos Sci Technol 2009;69:2064–8. https://doi.org/10.1016/j.compscitech.2008.08.016.
[6] Mallikarachchi HMYC, Pellegrino S. Quasi-static folding and deployment of ultrathin composite tape-spring hinges. J Spacecr Rockets 2011;48:187–98. https://doi.org/10.2514/1.47321.
[7] Johannisson W, Harnden R, Zenkert D, Lindbergh G. Shape-morphing carbon fiber composite using electrochemical actuation. Proc Natl Acad Sci 2020;117:7658–64. https://doi.org/10.1073/pnas.1921132117.
[8] Sakovsky M, Bichara RM, Tawk Y, Costantine J. Enhancing multi-stability in helical lattices for adaptive structures. In: AIAA SCITECH 2022 Forum, American Institute of Aeronautics and Astronautics; 2021. doi: 10.2514/6.2022-0923.
[9] Rodriguez JN, Zhu C, Duoss EB, Wilson TS, Spadaccini CM, Lewicki JP. Shape-morphing composites with designed micro-architectures. Sci Rep 2016;6:27933. https://doi.org/10.1038/srep27933.
[10] Crawley EF, de Luis J. Use of piezoelectric actuators as elements of intelligent structures. AIAA J 1987;25:1373–85. https://doi.org/10.2514/3.9792.
[11] Malakooti MH, Patterson BA, Hwang H-S, Sodano HA. ZnO nanowire interfaces for high strength multifunctional composites with embedded energy harvesting. Energy Environ Sci 2016;9:634–43. https://doi.org/10.1039/c5ee03181h.
[12] de Luzuriaga AR, Martin R, Markaide N, Rekondo A, Cabañero G, Rodríguez J, et al. Epoxy resin with exchangeable disulfide crosslinks to obtain reprocessable, repairable and recyclable fiber-reinforced thermoset composites. Mater Horiz 2016;3:241–7. https://doi.org/10.1039/C6MH00029K.
[13] Güemes A, Fernandez-Lopez A, Pozo AR, Sierra-Pérez J. Structural health monitoring for advanced composite structures: a review. J Compos Sci 2020;4:13. https://doi.org/10.3390/jcs4010013.
[14] de Oliveira R, Marques AT. Health monitoring of FRP using acoustic emission and artificial neural networks. Comput Struct 2008;86:367–73. https://doi.org/10.1016/j.compstruc.2007.02.015.
[15] Böger L, Wichmann MHG, Meyer LO, Schulte K. Load and health monitoring in glass fibre reinforced composites with an electrically conductive nanocomposite epoxy matrix. Compos Sci Technol 2008;68:1886–94. https://doi.org/10.1016/j.compscitech.2008.01.001.
[16] Lau K, Yuan L, Zhou L, Wu J, Woo C. Strain monitoring in FRP laminates and concrete beams using FBG sensors. Compos Struct 2001;51:9–20. https://doi.org/10.1016/S0263-8223(00)00094-5.
[17] Bekas DG, Tsirka K, Baltzis D, Paipetis AS. Self-healing materials: a review of advances in materials, evaluation, characterization and monitoring techniques.

Compos Part B Eng 2016;87:92–119. https://doi.org/10.1016/j.compositesb.2015.09.057.
[18] Kadam S, Chavan S, Kanu NJ. An insight into advance self-healing composites. Mater Res Exp 2021;8:052001. https://doi.org/10.1088/2053-1591/abfba5.
[19] van der Zwaag S, Grande AM, Post W, Garcia SJ, Bor TC. Review of current strategies to induce self-healing behaviour in fibre reinforced polymer based composites. Mater Sci Technol 2014;30:1633–41. https://doi.org/10.1179/1743284714Y.0000000624.
[20] Paolillo S, Bose RK, Santana MH, Grande AM. Intrinsic self-healing epoxies in Polymer Matrix Composites (PMCs) for aerospace applications. Polymers 2021;13:201. https://doi.org/10.3390/polym13020201.
[21] Madara SR, Raj NSS, Selvan CP. Review of research and developments in self healing composite materials. IOP Conf Ser Mater Sci Eng 2018;346:012011. https://doi.org/10.1088/1757-899X/346/1/012011.
[22] White SR, Sottos NR, Geubelle PH, Moore JS, Kessler MR, Sriram SR, et al. Autonomic healing of polymer composites. Nature 2001;409:794–7. https://doi.org/10.1038/35057232.
[23] Patrick JF, Hart KR, Krull BP, Diesendruck CE, Moore JS, White SR, et al. Continuous self-healing life cycle in vascularized structural composites. Adv Mater 2014;26:4302–8. https://doi.org/10.1002/adma.201400248.
[24] Esser-Kahn AP, Thakre PR, Dong H, Patrick JF, Vlasko-Vlasov VK, Sottos NR, et al. Three-dimensional microvascular fiber-reinforced composites. Adv Mater 2011;23:3654–8. https://doi.org/10.1002/adma.201100933.
[25] Azcune I, Odriozola I. Aromatic disulfide crosslinks in polymer systems: Self-healing, reprocessability, recyclability and more. Eur Polym J 2016;84:147–60. https://doi.org/10.1016/j.eurpolymj.2016.09.023.
[26] Grande AM, Martin R, Odriozola I, van der Zwaag S, Garcia SJ. Effect of the polymer structure on the viscoelastic and interfacial healing behaviour of poly (urea-urethane) networks containing aromatic disulphides. Eur Polym J 2017;97:120–8. https://doi.org/10.1016/j.eurpolymj.2017.10.007.
[27] Meure S, Furman S, Khor S. Poly[ethylene-co-(methacrylic acid)] healing agents for mendable carbon fiber laminates. Macromol Mater Eng 2010;295:420–4. https://doi.org/10.1002/mame.200900345.
[28] Ladani RB, Pingkarawat K, Nguyen ATT, Wang CH, Mouritz AP. Delamination toughening and healing performance of woven composites with hybrid z-fibre reinforcement. Compos Part Appl Sci Manuf 2018;110:258–67. https://doi.org/10.1016/j.compositesa.2018.04.028.
[29] Snyder AD, Phillips ZJ, Turicek JS, Diesendruck CE, Nakshatrala KB, Patrick JF. Prolonged in situ self-healing in structural composites via thermo-reversible entanglement. Nat Commun 2022;13:6511. https://doi.org/10.1038/s41467-022-33936-z.
[30] Shrivastava R, Singh KK. Interlaminar fracture toughness characterization of laminated composites: a review. Polym Rev 2020;60:542–93. https://doi.org/10.1080/15583724.2019.1677708.
[31] Nakajima K, Utsumi N, Saito Y, Yoshida M. Deformation property and suppression of ultra-thin-walled rectangular tube in rotary draw bending. Metals 2020;10:1074. https://doi.org/10.3390/met10081074.
[32] Dry C. Self-repairing composites for airplane components. Sens Smart Struct Technol Civ Mech Aerosp Syst; vol. 6932, International Society for Optics and Photonics; 2008, p. 693212. doi: 10.1117/12.776497.
[33] Benazzo F, Sodano HA. Evaluation of interfacial shear strength healing efficiency between dynamic covalent bond-based epoxy and functionalized fiberglass n.d.: 10.
[34] Aïssa B, Therriault D, Haddad E, Jamroz W. Self-healing materials systems: overview of major approaches and recent developed technologies. Adv Mater Sci Eng 2012;2012:e854203.
[35] Qamar IPS, Sottos NR, Trask RS. Grand challenges in the design and manufacture of vascular self-healing. Multifunct Mater 2020;3:013001. https://doi.org/10.1088/2399-7532/ab69e2.
[36] Kessler MR, White SR. Self-activated healing of delamination damage in woven composites. Compos Part Appl Sci Manuf 2001;32:683–99. https://doi.org/10.1016/S1359-835X(00)00149-4.
[37] Varley RJ, Parn GP. Thermally activated healing in a mendable resin using a non woven EMAA fabric. Compos Sci Technol 2012;72:453–60. https://doi.org/10.1016/j.compscitech.2011.12.007.
[38] Bekas DG, Baltzis D, Paipetis AS. Nano-reinforced polymeric healing agents for vascular self-repairing composites. Mater Des 2017;116:538–44. https://doi.org/10.1016/j.matdes.2016.12.049.
[39] Kostopoulos V, Kotrotsos A, Tsokanas P, Tsantzalis S. Toughening and healing of composites by CNTs reinforced copolymer nylon micro-particles. Mater Res Exp 2018;5:025305. https://doi.org/10.1088/2053-1591/aaabfb.
[40] Kotrotsos A, Kostopoulos V. 18 - Self-healing of structural composites containing common thermoplastics enabled or not by nanotechnology as healing agent. In: Khan A, Jawaid M, Raveendran SN, Ahmed Asiri AM, editors. Self-Heal. Compos. Mater., Woodhead Publishing; 2020. p. 327–74. doi: 10.1016/B978-0-12-817354-1.00018-1.
[41] Kessler MR, Sottos NR, White SR. Self-healing structural composite materials. Compos Part Appl Sci Manuf 2003;34:743–53. https://doi.org/10.1016/S1359-835X(03)00138-6.
[42] Yin T, Zhou L, Rong MZ, Zhang MQ. Self-healing woven glass fabric/epoxy composites with the healant consisting of micro-encapsulated epoxy and latent curing agent. Smart Mater Struct 2007;17:015019. https://doi.org/10.1088/0964-1726/17/01/015019.
[43] Wang CH, Sidhu K, Yang T, Zhang J, Shanks R. Interlayer self-healing and toughening of carbon fibre/epoxy composites using copolymer films. Compos Part Appl Sci Manuf 2012;43:512–8. https://doi.org/10.1016/j.compositesa.2011.11.020.
[44] Pingkarawat K, Wang CH, Varley RJ, Mouritz AP. Self-healing of delamination cracks in mendable epoxy matrix laminates using poly[ethylene-co-(methacrylic acid)] thermoplastic. Compos Part Appl Sci Manuf 2012;43:1301–7. https://doi.org/10.1016/j.compositesa.2012.03.010.
[45] Coope TS, Wass DF, Trask RS, Bond IP. Metal triflates as catalytic curing agents in self-healing fibre reinforced polymer composite materials. Macromol Mater Eng 2014;299:208–18. https://doi.org/10.1002/mame.201300026.
[46] Manfredi E, Cohades A, Richard I, Michaud V. Assessment of solvent capsule-based healing for woven E-glass fibre-reinforced polymers. Smart Mater Struct 2014;24:015019. https://doi.org/10.1088/0964-1726/24/1/015019.
[47] Fleet EJ, Zhang Y, Hayes SA, Smith PJ. Inkjet printing of self-healing polymers for enhanced composite interlaminar properties. J Mater Chem A 2015;3:2283–93. https://doi.org/10.1039/C4TA05422A.
[48] Aniskevich A, Vidinejevs S, Kulakov V, Strekalova O. Development of composites with a self-healing function. Mater Sci 2015;21:32–7. https://doi.org/10.5755/j01.ms.21.1.5354.
[49] Heo Y, Sodano HA. Thermally responsive self-healing composites with continuous carbon fiber reinforcement. Compos Sci Technol 2015;118:244–50. https://doi.org/10.1016/j.compscitech.2015.08.015.
[50] Kostopoulos V. Mode II fracture toughening and healing of composites using supramolecular polymer interlayers. Express Polym Lett 2016;10:914–26. https://doi.org/10.3144/expresspolymlett.2016.85.
[51] Kostopoulos V, Kotrotsos A, Tsantzalis S, Tsokanas P, Loutas T, Bosman AW. Toughening and healing of continuous fibre reinforced composites by supramolecular polymers. Compos Sci Technol 2016;128:84–93. https://doi.org/10.1016/j.compscitech.2016.03.021.
[52] Pingkarawat K, Dell'Olio C, Varley RJ, Mouritz AP. Poly(ethylene-co-methacrylic acid) (EMAA) as an efficient healing agent for high performance epoxy networks using diglycidyl ether of bisphenol A (DGEBA). Polymer 2016;92:153–63. https://doi.org/10.1016/j.polymer.2016.03.054.
[53] Ghazali H, Ye L, Zhang MQ. Interlaminar fracture of CF/EP composite containing a dual-component microencapsulated self-healant. Compos Part Appl Sci Manuf 2016;82:226–34. https://doi.org/10.1016/j.compositesa.2015.12.012.
[54] Kostopoulos V, Kotrotsos A, Tsantzalis S, Tsokanas P, Christopoulos AC, Loutas T. Toughening and healing of continuous fibre reinforced composites with bis-maleimide based pre-pregs. Smart Mater Struct 2016;25:084011. https://doi.org/10.1088/0964-1726/25/8/084011.
[55] Bolimowski PA, Wass DF, Bond IP. Assessment of microcapsule—catalyst particles healing system in high performance fibre reinforced polymer composite. Smart Mater Struct 2016;25:084009. https://doi.org/10.1088/0964-1726/25/8/084009.
[56] Ghazali H, Ye L, Zhang MQ. Mode II interlaminar fracture toughness of CF/EP composite containing microencapsulated healing resins. Compos Sci Technol 2017;142:275–85. https://doi.org/10.1016/j.compscitech.2017.02.018.
[57] Cohades A, Michaud V. Thermal mending in E-glass reinforced poly (ε-caprolactone)/epoxy blends. Compos Part Appl Sci Manuf 2017;99:129–38. https://doi.org/10.1016/j.compositesa.2017.04.013.
[58] Narducci F, Lee K-Y, Pinho ST. Interface micro-texturing for interlaminar toughness tailoring: a film-casting technique. Compos Sci Technol 2018;156:203–14. https://doi.org/10.1016/j.compscitech.2017.10.016.
[59] Zhang L, Tian X, Malakooti MH, Sodano HA. Novel self-healing CFRP composites with high glass transition temperatures. Compos Sci Technol 2018;168:96–103. https://doi.org/10.1016/j.compscitech.2018.09.008.
[60] Jony B, Thapa M, Mulani SB, Roy S. Repeatable self-healing of thermosetting fiber reinforced polymer composites with thermoplastic healant. Smart Mater Struct 2019;28:025037. https://doi.org/10.1088/1361-665X/aaf833.
[61] Gao Y, Liu L, Wu Z, Zhong Z. Toughening and self-healing fiber-reinforced polymer composites using carbon nanotube modified poly (ethylene-co-methacrylic acid) sandwich membrane. Compos Part Appl Sci Manuf 2019;124:105510. https://doi.org/10.1016/j.compositesa.2019.105510.
[62] Thapa M, Jony B, Mulani SB, Roy S. Experimental characterization of shape memory polymer enhanced thermoplastic self-healing carbon/epoxy composites. In: AIAA Scitech 2019 Forum, American Institute of Aeronautics and Astronautics; 2019. https://doi.org/10.2514/6.2019-1112.
[63] Shanmugam L, Naebe M, Kim J, Varley RJ, Yang J. Recovery of Mode I self-healing interlaminar fracture toughness of fiber metal laminate by modified double cantilever beam test. Compos Commun 2019;16:25–9. https://doi.org/10.1016/j.coco.2019.08.009.
[64] Loh TW, Ladani RB, Orifici A, Kandare E. Ultra-tough and in-situ repairable carbon/epoxy composite with EMAA. Compos Part Appl Sci Manuf 2021;143:106206. https://doi.org/10.1016/j.compositesa.2020.106206.
[65] Tsilimigkra X, Bekas D, Kosarli M, Tsantzalis S, Paipetis A, Kostopoulos V. Mechanical properties assessment of low-content capsule-based self-healing structural composites. Appl Sci Switz 2020;10. https://doi.org/10.3390/APP10175739.
[66] Kato Y, Minakuchi S, Ogihara S, Takeda N. Self-healing composites structure using multiple through-thickness microvascular channels. Adv Compos Mater 2020:1–18. https://doi.org/10.1080/09243046.2020.1744228.
[67] Jony B, Mulani SB, Mode II RS. Fracture toughness recovery of CFRP composite using thermoplastic shape memory polymer healant. In: AIAA Scitech 2020 Forum, American Institute of Aeronautics and Astronautics; 2020. https://doi.org/10.2514/6.2020-1388.

[68] D'Elia E, Eslava S, Miranda M, Georgiou TK, Saiz E. Autonomous self-healing structural composites with bio-inspired design. Sci Rep 2016;6:25059. https://doi.org/10.1038/srep25059.

[69] Elhadary M, Hamdy A, Shaker W. Effect of fiber bridging in composites healing. Alex Eng J 2022;61:2769–74. https://doi.org/10.1016/j.aej.2021.08.002.

[70] Liu JL, Lee HP, Tay TE, Tan VBC. Healable bio-inspired helicoidal laminates. Compos Part Appl Sci Manuf 2020;137:106024. https://doi.org/10.1016/j.compositesa.2020.106024.

[71] Benazzo F, Rigamonti D, Bettini P, Sala G, Grande AM. Interlaminar fracture of structural fibre/epoxy composites integrating damage sensing and healing. Compos Part B Eng 2022;244:110137. https://doi.org/10.1016/j.compositesb.2022.110137.

[72] Sridharan S. Delamination Behaviour of Composites; 2008. doi: 10.1533/9781845694821.

[73] Arrese A, Mujika F. Influence of bending rotations on three and four-point bend end notched flexure tests. Eng Fract Mech 2008;75:4234–46. https://doi.org/10.1016/j.engfracmech.2008.03.012.

[74] Zile E, Tamuzs V. Mode II delamination of a unidirectional carbon fiber/epoxy composite in four-point bend end-notched flexure tests. Mech Compos Mater 2005;41:383–90. https://doi.org/10.1007/s11029-005-0064-2.

[75] Jony B, Roy S, Mulani SB. Fracture resistance of in-situ healed CFRP composite using thermoplastic healants. Mater Today Commun 2020;24:101067. https://doi.org/10.1016/j.mtcomm.2020.101067.

[76] Irwin GR. Fracture. In: Flügge S, editor. Elast Plast Elastizität Plast, Berlin, Heidelberg: Springer; 1958, p. 551–90. doi: 10.1007/978-3-642-45887-3_5.

[77] Cohades A, Hostettler N, Pauchard M, Plummer CJG, Michaud V. Stitched shape memory alloy wires enhance damage recovery in self-healing fibre-reinforced polymer composites. Compos Sci Technol 2018;161:22–31. https://doi.org/10.1016/j.compscitech.2018.03.040.

[78] Park JS, Darlington T, Starr AF, Takahashi K, Riendeau J, Thomas HH. Multiple healing effect of thermally activated self-healing composites based on Diels-Alder reaction. Compos Sci Technol 2010;70:2154–9. https://doi.org/10.1016/j.compscitech.2010.08.017.

[79] Serafinavicius T, Kvedaras AK, Sauciuvenas G. Bending behavior of structural glass laminated with different interlayers. Mech Compos Mater 2013;49:437–46. https://doi.org/10.1007/s11029-013-9360-4.

[80] Morrell R. Measurement Good Practice Guide No. 7 n.d.:74.

[81] O'brien K, Johnston W, Toland G. NASA Technical Reports Server (NTRS). n.d.

[82] Carlsson L, Gillespie Jr J, Pipes B. On the analysis and design of the End Notched Flexure (ENF) specimen for mode II testing. J Compos Mater 1986;20. https://doi.org/10.1177/002199838602000606.

[83] Wang W-X, Nakata M, Takao Y, Matsubara T. Experimental investigation on test methods for mode II interlaminar fracture testing of carbon fiber reinforced composites. Compos Part Appl Sci Manuf 2009;40:1447–55. https://doi.org/10.1016/j.compositesa.2009.04.029.

[84] Pérez-Galmés M, Renart J, Sarrado C, Brunner AJ, Rodríguez-Bellido A. Towards a consensus on mode II adhesive fracture testing: experimental study. Theor Appl Fract Mech 2018;98:210–9. https://doi.org/10.1016/j.tafmec.2018.09.014.

[85] de Oliveira BMA, Campilho RDSG, Silva FJG, Rocha RJB. Comparison between the ENF and 4ENF fracture characterization tests to evaluate GIIC of bonded aluminium joints. J Adhes 2018;94:910–31. https://doi.org/10.1080/00218464.2017.1387056.

[86] Martin Rh, Davidson Bd. Mode II fracture toughness evaluation using four point bend, end notched flexure test. Plast Rubber Compos 1999;28:401–6. https://doi.org/10.1179/146580199101540565.

[87] Davidson BD, Sun X, Vinciquerra AJ. Influences of friction, geometric nonlinearities, and fixture compliance on experimentally observed toughnesses from three and four-point bend end-notched flexure tests. J Compos Mater 2007;41:1177–96. https://doi.org/10.1177/0021998306067304.

[88] The analysis of interlaminar fracture in uniaxial fibre-polymer composites. Proc R Soc Lond Math Phys Sci; 1990. doi: 10.1098/rspa.1990.0007.

[89] Liu W, Chen P. A simple procedure for the determination of the cohesive law in 4-ENF test with consideration of the friction and R-curve effect. Eng Fract Mech 2019;220:106651. https://doi.org/10.1016/j.engfracmech.2019.106651.

[90] Konlan J, Mensah P, Ibekwe S, Crosby K, Li G. Vitrimer based composite laminates with shape memory alloy Z-pins for repeated healing of impact induced delamination. Compos Part B Eng 2020;200:108324. https://doi.org/10.1016/j.compositesb.2020.108324.

[91] Liu Y, Budhlall BM. Self-healing nanocomposites comprised of poly(urea formaldehyde) nanocapsules in a thermosetting polyurea. Eur Polym J 2020;126:109545. https://doi.org/10.1016/j.eurpolymj.2020.109545.

[92] Trask RS, Norris CJ, Bond IP. Stimuli-triggered self-healing functionality in advanced fibre-reinforced composites. J Intell Mater Syst Struct 2013. https://doi.org/10.1177/1045389X13505006.

[93] Norris CJ, Bond IP, Trask RS. Healing of low-velocity impact damage in vascularised composites. Compos Part Appl Sci Manuf 2013;44:78–85. https://doi.org/10.1016/j.compositesa.2012.08.022.

[94] Patel AJ, Sottos NR, Wetzel ED, White SR. Autonomic healing of low-velocity impact damage in fiber-reinforced composites. Compos Part Appl Sci Manuf 2010;41:360–8. https://doi.org/10.1016/j.compositesa.2009.11.002.

[95] Liu JL, Mencattelli L, Zhi J, Chua PY, Tay T-E, Tan VBC. Lightweight, fiber-damage-resistant, and healable bio-inspired glass-fiber reinforced polymer laminate. Polymers 2022;14:475. https://doi.org/10.3390/polym14030475.

[96] Feng X, Li G. Room-temperature self-healable and mechanically robust thermoset polymers for healing delamination and recycling carbon fibers. ACS Appl Mater Interfaces 2021;13:53099–110. https://doi.org/10.1021/acsami.1c16105.

[97] Bond IP, Williams GJ, Trask RS. Self-healing CFRP for aerospace applications: 16th international conference on composite materials, ICCM-16 – "a giant step towards environmental awareness: from green composites to aerospace." ICCM Int Conf Compos Mater; 2007.

[98] Hart KR, Wetzel ED, Sottos NR, White SR. Self-healing of impact damage in fiber-reinforced composites. Compos Part B Eng 2019;173:106808. https://doi.org/10.1016/j.compositesb.2019.05.019.

[99] Wang H, Chang L, Ye L, Williams GJ. Micro-cutting tests: a new way to measure the fracture toughness and yield stress of polymeric nanocomposites. In: 13th int conf fract 2013 ICF 2013 2013;4:3419–24.

[100] Chen B, Cai H, Mao C, Gan Y, Wei Y. Toughening and rapid self-healing for carbon fiber/epoxy composites based on electrospinning thermoplastic polyamide nanofiber. Polym Compos n.d.;n/a. doi: 10.1002/pc.26605.

[101] Azevedo do Nascimento A, Fernandez FS, da Silva FPC, Ferreira ED, Melo JD, Cysne Barbosa AP. Addition of poly (ethylene-co-methacrylic acid) (EMAA) as self-healing agent to carbon-epoxy composites. Compos Part Appl Sci Manuf 2020;137:106016. https://doi.org/10.1016/j.compositesa.2020.106016.

[102] Hosseini MR, Taheri-Behrooz F, Salamat-talab M. Mode II interlaminar fracture toughness of woven E-glass/epoxy composites in the presence of mat interleaves. Int J Adhes Adhes 2020;98:102523. https://doi.org/10.1016/j.ijadhadh.2019.102523.

[103] Callister W, Rethwish D. Ch 8. Failure. Mater. Sci. Eng. Introd. 10th Ed. Wiley, n.d.

[104] Lagunegrand L, Lorriot Th, Harry R, Wargnier H. Design of an improved four point bending test on a sandwich beam for free edge delamination studies. Compos Part B Eng 2005;37:127–36. https://doi.org/10.1016/j.compositesb.2005.07.002.

[105] Carlsson LA, Adams DF, Pipes RB. Experimental characterization of advanced composite materials. 4th ed. CRC Press; 2014.

[106] Brown EN, Sottos NR, White SR. Fracture testing of a self-healing polymer composite. Exp Mech 2002;42:372–9. https://doi.org/10.1007/BF02412141.

[107] Gentile D. Experimental characterization of interlaminar fracture toughness of composite laminates assembled with three different carbon fiber lamina. Frat Ed Integrità Strutt 2018;12:155–70. https://doi.org/10.3221/IGF-ESIS.43.12.

[108] Awerbuch J, Leone FA, Ozevin D, Tan T-M. On the applicability of acoustic emission to identify modes of damage in full-scale composite fuselage structures. J Compos Mater 2016;50:447–69. https://doi.org/10.1177/0021998315576379.

[109] Linde P, de Boer H. Modelling of inter-rivet buckling of hybrid composites. Compos Struct 2006;73:221–8. https://doi.org/10.1016/j.compstruct.2005.11.062.

[110] Zimmermann N, Wang PH. A review of failure modes and fracture analysis of aircraft composite materials. Eng Fail Anal 2020;115:104692. https://doi.org/10.1016/j.engfailanal.2020.104692.